

Supplementary Information

Ultra-facile Aqueous Synthesis of Nanoporous Zeolitic Imidazolate Framework Membranes for Hydrogen Purification and Olefin/paraffin separation

Xu Jiang, Songwei Li, Yongping Bai and Lu Shao*

MIIT Key Laboratory of Critical Materials Technology for New Energy Conversion and Storage, State Key Laboratory of Urban Water Resource and Environment School of Chemistry and Chemical Engineering, Harbin Institute of Technology, Harbin 150001, PR China.

Email: shaolu@hit.edu.cn

ESI Content

Fig. S1. Digital images and schematic drawing of the apparatus for membrane preparation.

Fig. S2. Constant-volume apparatus for single gas permeation test.

Fig. S3. The propylene/propane binary gas permeation measurement set up.

Fig. S4. SEM images of ZIF-8/PDA-24 membrane.

Fig. S5. SEM images of pure ZIF-8 deposited on AAO

Fig. S6. FT-IR spectra of ZIF-8/PDA membranes and PDA coated AAO.

Fig. S7. TGA curves of particles collected from ZIF-8 precursor solution and ZIF-8/DA precursor solution.

Fig. S8. FT-IR spectra of particles collected from ZIF-8 reaction solution and ZIF-8/DA reaction solution.

Fig. S9. The solution pH as a function of synthesis period.

Fig. S10. Comparison of the ZIF-8 membrane with the theoretical ZIF-8 permeability.

Fig. S11. SEM images of ZIF-8/PDA-12 on CA micro-filtration membrane.

Fig. S12. SEM images of ZIF-8/PDA-12 on Polyimide nano-filtration membrane.

Table S1. Element mass concentration of pure ZIF-8 and ZIF-8/PDA membranes.

Table S2. Gas permeance and selectivity of ZIF-8/PDA membranes.

Table S3. Comparison of the gas separation performances of the ZIF-8 membrane in this study with other molecular sieving membranes from literatures.

Table S4. The propylene/propane binary gas permeance and selectivity of ZIF-8/DA membranes.

Materials.

Zn (NO₃)₂·6H₂O, 2-methylimidazole, and dopamine hydrochloride were purchased from Sigma-Aldrich(Shanghai) Trading Co., Ltd. (Shanghai, China). Anodisc 25 (0.02um) were obtained from Whatman™

Membrane preparation

Here, we used a common sand core filter as the equipment for membrane preparation (**Fig. S1a**). Generally, the sand core is porous so that the liquid can penetrate through it. During the membrane synthesis, the sand core is sealed by plastic wrap to prevent the liquid leak. The AAO plate is placed right on the wrapped sand core, then put on the cylindrical funnel and sealed the seams, thus the equipment for membrane preparation is ready (**Fig. S1b**). When we start to grow ZIF-8 membrane, just pure the precursor solution into the cylindrical funnel, and keep the whole apparatus standing for a certain period. During the whole process, we didn't use the filtering capability of the sand core filter so that no actual vacuum is applied. the sand core filter just served as a support for AAO to keep the reaction solution only on the top side of AAO. Other equipment which could offer similar benefit can also be used.

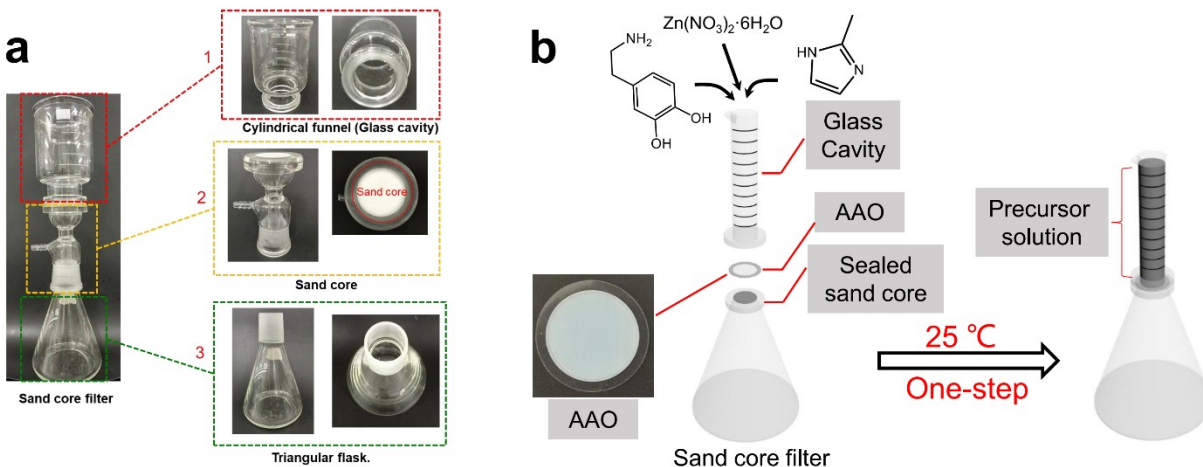


Fig. S1. a) Digital images of sand core filter. 1. Cylindrical funnel (glass cavity); 2. Sand core; 3. Triangular flask.
b) Schematic drawing of the sand core filter for the simple one-step membrane preparation

Gas permeation test.

Single gas test.

The single gas permeation of membranes was measured using a homemade constant-volume apparatus(**Fig. S2**). Membranes were sealed on a stainless steel permeation cell with aluminum tape with an effective test area of 0.79 cm². The feed pressure of each testing gas is atmospheric pressure. And the gases were test in the sequence of H₂, CO₂, N₂, CH₄, C₃H₆ and C₃H₈ at 35 °C.

The molar flow rate (N_a) of the permeating gas was calculated from the linear pressure rise, and its coefficient was calibrated using a digital flowmeter Membrane permeance P_a (mol·m⁻²·s⁻¹·Pa⁻¹) could be calculated with the following equation 1.

$$P_a = \frac{N_a}{\Delta P \times A} \quad (1)$$

where N_a (mol·s⁻¹) is the permeate flow rate of component gas a, ΔP_a (P_a) is the pressure difference of upstream and downstream of the membrane, and A (m²) is the membrane area. The ideal selectivity of gas to gas b (S_{a/b}) were calculated from P_a and P_b as shown in equation 2.

$$S_{a/b} = \frac{P_a}{P_b} \quad (2)$$

The permeance of all gases could be converted to permeability, Since the unit of permeance is mol m⁻² s⁻¹ Pa⁻¹, while 1 Barrer = 3.4 × 10⁻¹⁵ mol · m · m⁻² · s⁻¹ · Pa⁻¹ Therefore, the permeance-permeability conversion equation can be expressed as follow:

$$P_1 = \frac{3.4 \times P_2}{l} \quad (3)$$

Where P_1 is permeance ($\text{mol} \cdot \text{m}^{-2} \cdot \text{s}^{-1} \cdot \text{Pa}^{-1}$) data, P_2 is permeability ($10^{-10} \cdot \text{cm}^3(\text{STP}) \cdot \text{cm} \cdot \text{cm}^{-2}$) data, l (μm) is membrane thickness.

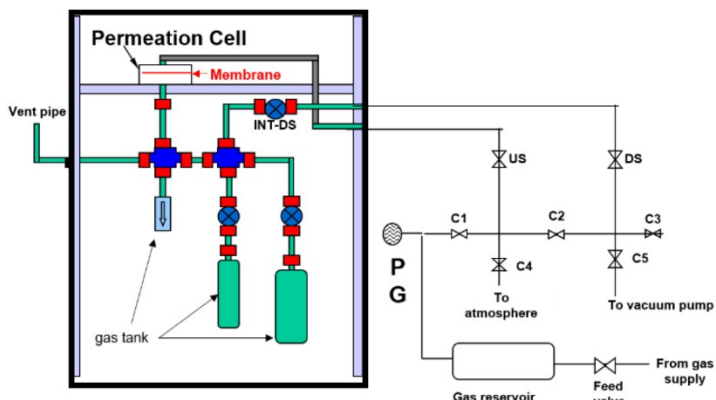


Fig. S2. Constant-volume apparatus for single gas permeation test.

Propylene/propane binary gas test

The binary gas measurements were conducted on a Wicke–Kallenbach setup (**Fig. S3**). Generally, the feed gas made of equimolar mixture of propylene/propane were fed to the top surface of the membrane while argon were used as the weep gas on the permeate side. The feed pressure was 1 atm. The total flux of the permeate gas were measured by a flow meter and the composition was analyzed by a gas chromatography (EchromA90).

The separation factor $S_{i/j}$ of a binary mixture permeation is defined as the quotient of the molar ratios of the components(i,j) in the permeate, divided by the quotient of the molar ratio of the components(i,j) in the retentate as shown in following equation 3.

$$S_{i/j} = \frac{y_{i, \text{Perm}}/y_{j, \text{Perm}}}{y_{i, \text{Ret}}/y_{j, \text{Ret}}} \quad (3)$$

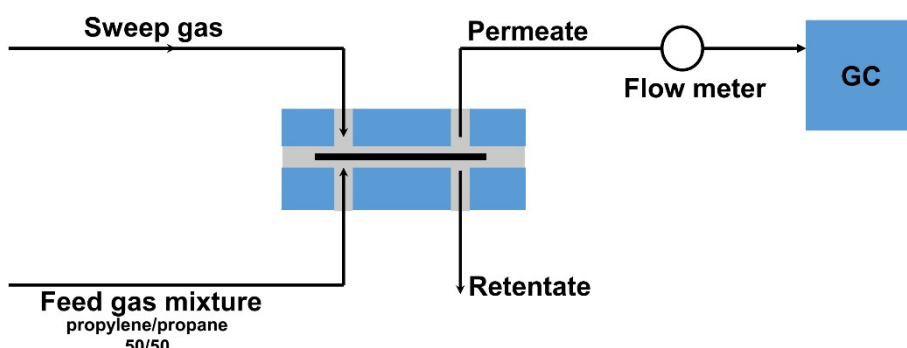


Fig. S3. The propylene/propane binary gas permeation measurement set up.

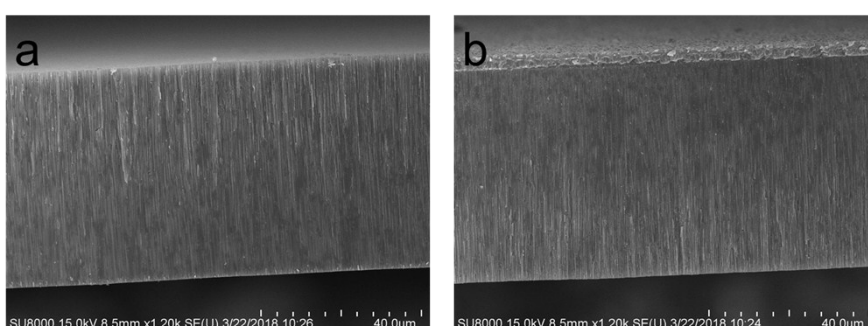


Fig. S4. SEM cross-sectional view of a) AAO support and b) as-prepared ZIF-8/PDA-24 membrane.

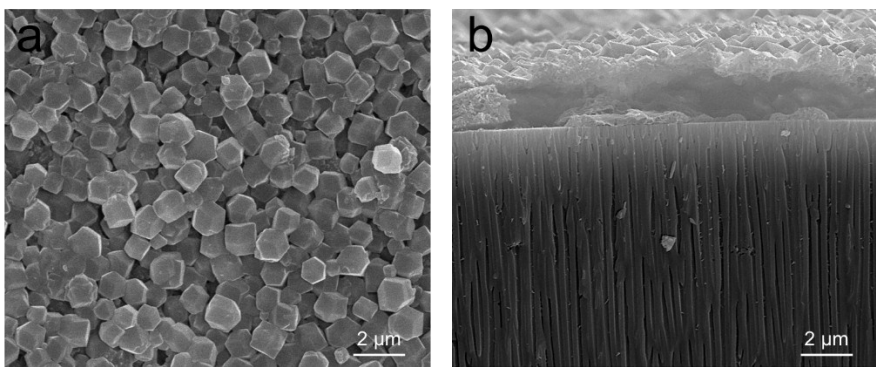


Fig. S5. SEM images of pure ZIF-8 deposited on AAO support a) top view, b) cross-sectional view.

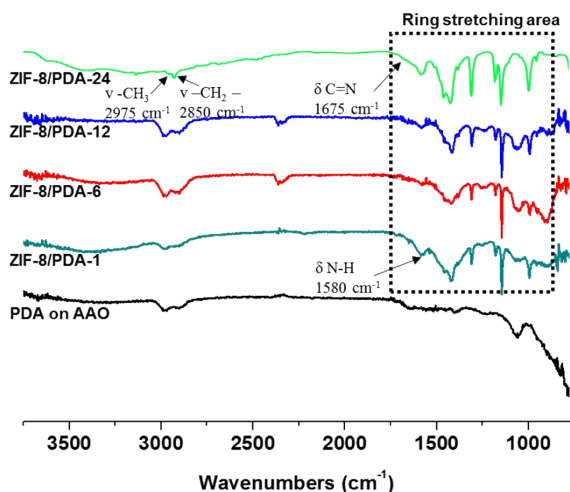


Fig. S6. FT-IR spectra of ZIF-8/PDA membranes and PDA coated AAO.

Pure PDA coated AAO shows weak absorption peaks while ZIF-8/PDA membranes show typical absorption peaks of Hmim ring streching accordding to the literature¹.

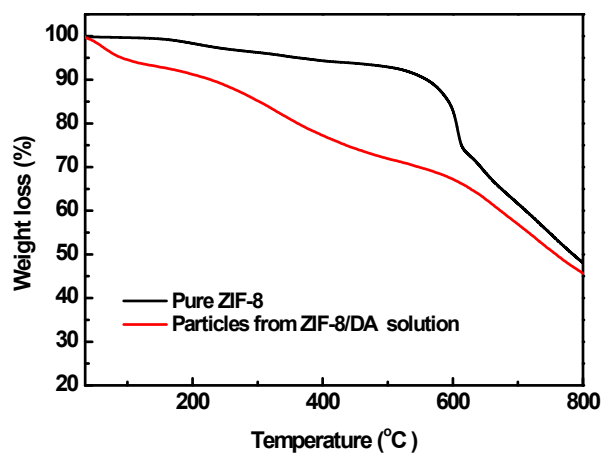


Fig. S7. TGA curves of particles collected from ZIF-8 precursor solution and ZIF-8/DA precursor solution.

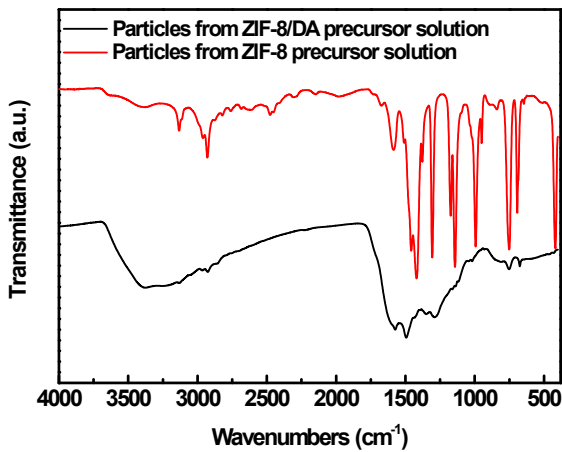


Fig. S8. FT-IR spectra of particles collected from ZIF-8 reaction solution and ZIF-8/DA reaction solution.

The FT-IR spectrum of particles from the ZIF-8/DA precursor solution shows identical peaks to pure polydopamine².

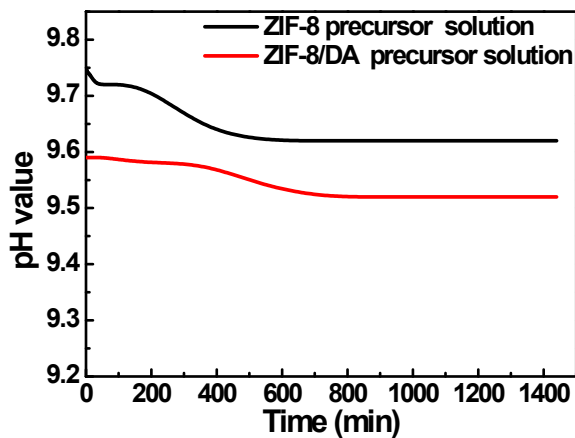


Fig. S9 The solution pH as a function of synthesis period.

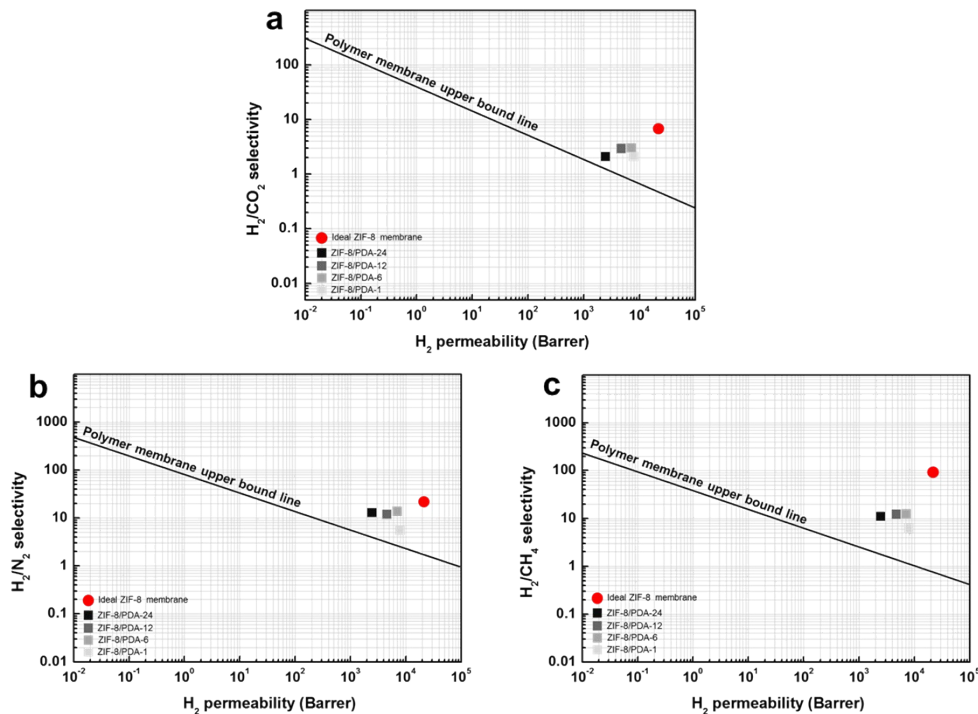


Fig. S10. Comparison of the ZIF-8 membrane with the theoretical ZIF-8 permeability. The black line denotes the Robeson upper bound for **b)** H_2/CO_2 , **c)** H_2/N_2 , and **d)** H_2/CH_4 . The ideal pure ZIF-8 permeability is based on gas adsorption test³.

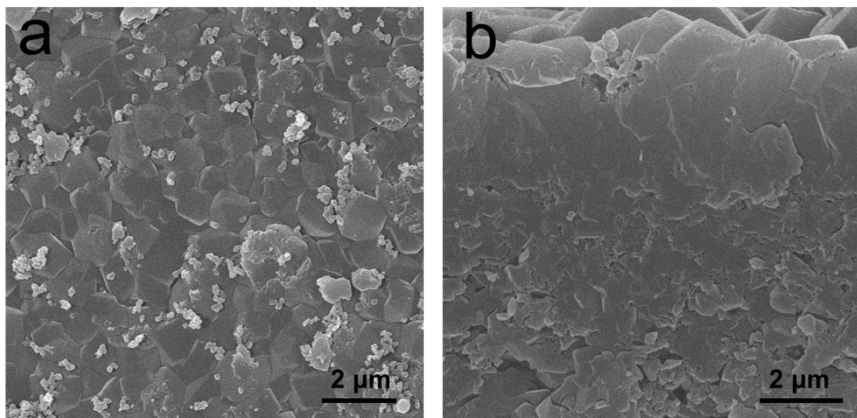


Fig. S11. SEM a) plain and b) cross-sectional images of ZIF-8/PDA-12 on CA micro-filtration membrane

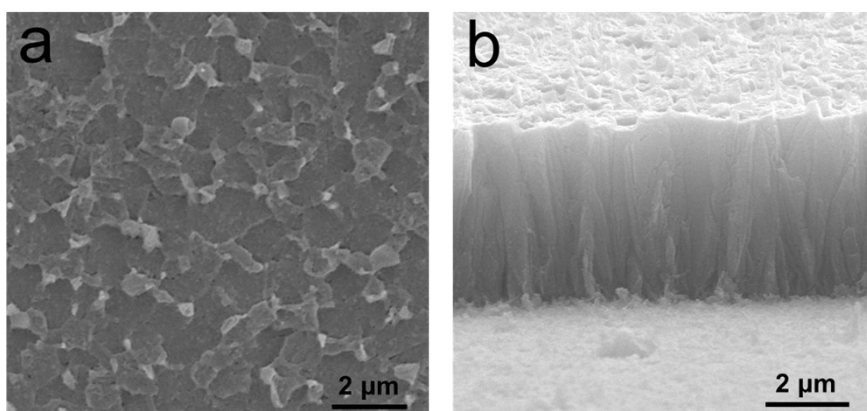


Fig. S12. SEM a) plain and b) cross-sectional images of ZIF-8/PDA-12 on Polyimide nano-filtration membrane

Our dopamine-assisted method can also synthesize ZIF-8/PDA membrane on polymer substrates such as cellulose acetate micro-filtration membrane and Polyimide nano-filtration membrane, suggesting the universality of this facile strategy for different substrate. Due to the different expansion rates in water, the polymeric substrates tend to severely shrink during the membrane drying process, resulting in the crack of ZIF-8 layer, thus the permeance data cannot be collected.

Table S1. Element mass concentration of pure ZIF-8 and ZIF-8/PDA membranes

Samples	N/Zn ratio	Atomic Concentration %				
		Zn 2p	O 1s	N 1s	C 1s	Al 2p
Pure ZIF-8 (Powder)	4.4	1.96	13.78	8.61	75.65	0.00
ZIF-8/PDA-1	4.6	3.03	10.42	14.00	72.54	0.00
ZIF-8/PDA-6	3.6	3.01	10.82	13.51	72.67	0.00
ZIF-8/PDA-12	2.5	4.89	18.00	12.24	64.86	0.00
ZIF-8/PDA-24	0.8	10.26	24.14	7.95	57.65	0.00

Table S2. Gas permeance and selectivity of ZIF-8/PDA membranes

Membrane	Thickness (μm)	Permeance (10^{-8} mol m $^{-2}$ s $^{-1}$ Pa $^{-1}$)							Selectivity				
		H ₂	CO ₂	N ₂	CH ₄	C ₃ H ₆	C ₃ H ₈	H ₂ /N ₂	H ₂ /CH ₄	H ₂ /C ₃ H ₆	H ₂ /C ₃ H ₈	C ₃ H ₆ /C ₃ H ₈	
ZIF-8/PDA-1	1.6 ±0.10	146 ±9.1	69.3 ±4.3	26.3 ±1.7	22.3 ±1.4	5.84 ±0.36	1.18 ±0.073	5.6 ±0.73	6.5 ±0.81	25.0 ±3.1	124 ±15.5	5.0 ±0.62	
ZIF-8/PDA-6	3.0 ±0.17	84.0 ±4.8	27.9 ±1.6	5.70 ±0.29	6.41 ±0.36	0.76 ±0.043	0.028 ±0.0015	14.7 ±1.9	13.1 ±1.5	110 ±12.5	3000 ±339	27.1 ±3.1	
ZIF-8/PDA-12	5.5 ±0.15	28.0 ±1.3	10.1 ±0.43	2.10 ±0.090	2.16 ±0.09	0.26 ±0.011	0.0041 ±0.00018	13.3 ±1.1	12.9 ±1.1	106 ±9.1	6680 ±572	63.1 ±5.4	
ZIF-8/PDA-24	6.8 ±0.50	12.3 ±0.91	6.41 ±0.47	0.85 ±0.063	1.00 ±0.074	0.19 ±0.013	0.0019 ±0.00014	14.4 ±2.1	12.3 ±1.8	65.6 ±9.6	6494 ±964	99.0 ±14.6	

Table S3. Comparison of the gas separation performances of the ZIF-8 membrane in this study with other molecular sieving membranes from literatures

Membrane	Substrate	Membrane Thickness (μm)	Temperature (°C) & Pressure (bar)	H ₂ Permeance (10 ⁻⁸ mol m ⁻² s ⁻¹ Pa ⁻¹)	Selectivity				Ref.
					H ₂ /N ₂	H ₂ /CH ₄	H ₂ /C ₃ H ₈	C ₃ H ₆ /C ₃ H ₈	
ZIF-8/PDA-1	AAO	1.6 ±0.10	35&1	146±9.1	5.6 ±0.73	6.5 ±0.81	124 ±15.5	5.0 ±0.62	This work
ZIF-8/PDA-6	AAO	3.0 ±0.17	35&1	84.0±4.8	14.7 ±1.9	13.1 ±1.5	3000 ±339	27.1 ±3.1	
ZIF-8/PDA-12	AAO	5.5 ±0.15	35&1	28.0±1.3	13.3 ±1.1	12.9 ±1.1	6680 ±572	63.1 ±5.4	
ZIF-8/PDA-24	AAO	6.8 ±0.50	35&1	12.3±0.91	14.4 ±2.1	12.3 ±1.8	6494 ±964	99.0 ±14.6	
ZIF-8/GO	AAO	~0.06	25&1	5.46	11.1	11.2	405.0	12	[4]
ZIF-8	titania	~40	25&1	6.04	11.6	12.6			[5]
ZIF-8	Al ₂ O ₃	~20	150&1	21.7	17.6	34.8	905.1	15.1	[6]
ZIF-8	Al ₂ O ₃	~2	25&1					~50	[7]
ZIF-8	PVDF	1<	25&1	2010	7.8	8.6			[8]
ZIF-8	α-alumina tubular	~1	25&1	23	13.7	14.8	953	36.0	[9]
ZIF-8	PVDF hollow fibre	0.017		2154	15.1	17.9	1145	44.5	[10]
ZIF-8	α-Al ₂ O ₃	~4	35&1	47.2	10.6	11.3		30.1	[11]
ZIF-8	AAO	2	25&1	768	9.4	14.2			[12]
ZIF-8	AAO	0.5	25&1	830	15.5	16.2	2655	31.6	[13]
ZIF-8/g-C ₃ N ₄	AAO	0.2	25&1	6.7		36	45	142	[14]
ZIF-8	Al ₂ O ₃		250&1	13	90	139.1	3816.6		[15]
ZIF-8	P84 HFs		35&1	1.3		72.4			[16]
ZIF-8	Ceramic tube	1.2						80	[17]
ZIF-8	AAO	0.2	25&1					300	[18]
ZIF-8	PTSC	0.62	25&0	21			1737	25.5	[19]
ZIF-8 coated with PTMSP	PTSC	1.4	25&0	11			4076	106	[19]
ZIF-7-8	Al ₂ O ₃		25&*	30	12.5	21.3			[20]
UiO-66	α-Al ₂ O ₃	5	25&1	2.6	4.7	12.9	22.4		[21]
ZIF-7	Al ₂ O ₃	1.5	200&1	8	7.7	5.9			[22]
ZIF-90	Al ₂ O ₃	20	200&1	25	12.6	15.9			[23]
NH ₂ -MIL-53	Glass frit discs	15	15&1	267.1	20.7	23.9			[24]
Cu ₃ (BTC) ₂	α-Al ₂ O ₃	13		7.25	7.18	5.80			[25]
JUC-150	nickel screen	30-40	25&1	18.3	17.1	26.1			[26]

Table S4. The propylene/propane binary gas permeance and selectivity of ZIF-8/DA membranes

Membrane	Permeance (10 ⁻¹⁰ mol m ⁻² s ⁻¹ Pa ⁻¹)		Selectivity
	C ₃ H ₆	C ₃ H ₈	
ZIF-8/PDA-1	553	148	3.74
ZIF-8/PDA-6	74.3	2.91	25.5
ZIF-8/PDA-12	25.5	0.44	58.0
ZIF-8/PDA-24	18.8	0.20	94.0

References:

- [1] M. Jian, B. Liu, G. Zhang, R. Liu, X. Zhang, *Colloids and Surfaces A: Physicochemical and Engineering Aspects* **2015**, 465, 67-76.
- [2] D. R. Dreyer, D. J. Miller, B. D. Freeman, D. R. Paul, C. W. Bielawski, *Langmuir* **2012**, 28, 6428-6435.
- [3] C. Zhang, R. P. Lively, K. Zhang, J. R. Johnson, O. Karvan, W. J. Koros, *J. Phys. Chem. Lett.* **2012**, 3, 2130-2134.
- [4] Y. Hu, J. Wei, Y. Liang, H. Zhang, X. Zhang, W. Shen, H. Wang, *Angew. Chem. Int. Ed.* **2016**, 55, 2048-2052.
- [5] H. Bux, F. Liang, Y. Li, J. Cravillon, M. Wiebcke, J. Caro, *J. Am. Chem. Soc.* **2009**, 131, 16000-16001.
- [6] Q. Liu, N. Wang, J. Caro, A. Huang, *J. Am. Chem. Soc.* **2013**, 135, 17679-17682.
- [7] H. T. Kwon, H. K. Jeong, *J. Am. Chem. Soc.* **2013**, 135, 10763-10768.
- [8] J. Hou, P. D. Sutrisna, Y. Zhang, V. Chen, *Angew. Chem. Int. Ed.* **2016**, 55, 3947-3951.
- [9] S. Tanaka, K. Okubo, K. Kida, M. Sugita, T. Takewaki, *J. Membr. Sci.* **2017**, 544, 306-311.
- [10] W. Li, P. Su, Z. Li, Z. Xu, F. Wang, H. Ou, J. Zhang, G. Zhang, E. Zeng, *Nat. Commun.* **2017**, 8, 406.
- [11] D. Liu, X. Ma, H. Xi, Y. S. Lin, *J. Membr. Sci.* **2014**, 451, 85-93.
- [12] P. Hu, Y. Yang, Y. Mao, J. Li, W. Cao, Y. Ying, Y. Liu, J. Lei and X. Peng, *CrystEngComm*, 2015, 17, 1576-1582.
- [13] G. He, M. Dakhchoune, J. Zhao, S. Huang and K. V. Agrawal, 2018, 28, 1707427.
- [14] J. Hou, Y. Wei, S. Zhou, Y. Wang and H. Wang, *Chemical Engineering Science*, 2018, 182, 180-188.
- [15] A. Huang, Q. Liu, N. Wang, Y. Zhu and J. Caro, *J. Am. Chem. Soc.*, 2014, 136, 14686-14689.
- [16] F. Cacho-Bailo, G. Caro, M. Etxeberria-Benavides, O. Karvan, C. Tellez and J. Coronas, *RSC Adv.*, 2016, 6, 5881-5889.
- [17] J. Sun, C. Yu and H.-K. Jeong, *Crystals*, 2018, 8, 373.
- [18] S. Zhou, Y. Wei, L. Li, Y. Duan, Q. Hou, L. Zhang, L.-X. Ding, J. Xue, H. Wang and J. Caro, 2018, 4, eaau1393.
- [19] E. Barankova, X. Tan, L. F. Villalobos, E. Litwiller, K. V. Peinemann, *Angew. Chem. Int. Ed.* **2017**, 56, 2965-2968.
- [20] F. Hillman, J. Brito, H. K. Jeong, *ACS Appl. Mater. Interfaces* **2018**, 10, 5586-5593.
- [21] S. Fribe, B. Geppert, F. Steinbach, J. Caro, *ACS Appl. Mater. Interfaces* **2017**, 9, 12878-12885.
- [22] Y. S. Li, F. Y. Liang, H. Bux, A. Feldhoff, W. S. Yang, J. Caro, *Angew. Chem. Int. Ed.* **2010**, 49, 548-551.
- [23] A. Huang, W. Dou, J. Caro, *J. Am. Chem. Soc.* **2010**, 132, 15562-15564.
- [24] F. Zhang, X. Zou, X. Gao, S. Fan, F. Sun, H. Ren, G. Zhu, *Adv. Funct. Mater.* **2012**, 22, 3583-3590.
- [25] S. Zhou, X. Zou, F. Sun, F. Zhang, S. Fan, H. Zhao, T. Schiestel, G. Zhu, *J. Mater. Chem.* **2012**, 22, 10322-10328.
- [26] Z. Kang, M. Xue, L. Fan, L. Huang, L. Guo, G. Wei, B. Chen, S. Qiu, *Energy Environ. Sci.* **2014**, 7, 4053-4060.